J Fluoresc (2014) 24:1087–1098
DOI 10.1007/s10895-014-1389-9

ORIGINAL PAPER

Fluorescent Styryl Dyes Based on Novel 4-Methoxy-9-Methyi-9H-Carbazole-3-Carbaldehyde—Synthesis, Photophysical Properties and DFT Computations

Prashant G. Umape · Yogesh Gawale · Nagaiyan Sekar

Received: 28 January 2014 / Accepted: 7 April 2014 / Published online: 1 May 2014
© Springer Science+Business Media New York 2014

Abstract Novel carbazole based styryl derivatives (**6a**–**6c**) having styryl group at third position and a methoxy substitution were synthesized by condensing 4-methoxy-9-methyl-9*H*-carbazole-3-carbaldehyde **3** and different active methylene derivatives (**5a**–**5c**). Evaluated photophysical properties of these synthesized novel chromophores, studied the effect of solvent polarity on absorption, emission and quantum yield of these styryl derivatives. DFT and TD-DFT computations are carried out to study structural, molecular, electronic and photophysical parameters of dyes. The ratio of ground state to excited state dipole moment was calculated using Bakhshiev and Kawski-Chamma-Viallet correlations.

Keywords Styryl compounds · Solid state fluorescence · Fluorescent · Solvatochromism · Solvatofluorism · TD-DFT

Introduction

The carbazole based molecular materials are electron rich and electrically active and are associated with small orbital overlaps in their n-π* transitions, leading to relatively small energy exchange [1]. Such materials are used in electroluminescent devices [2], light emitting diodes (LEDs) [3, 4], photorefractive materials [5], organic field effect transistors [6], and solar cells [7]. The carbazole based polymers are widely investigated as wide band gap energy transfer donor materials [8–11].

The dyes based on substituted carbazoles exhibit remarkable optical and electrical properties, due to which extensive research has been done on the synthesis and application of carbazole based dyes [12, 13]. Incorporation of a carbazole unit enhances thermal stability and fluorescence due to rigidity and planarity of the carbazole core and such molecules are used as probe materials for sensing pH, polarity, temperature as well as the microenvironment in supramolecular host cavities, micelles, polymers, and biomolecules [14].

The styryl derivatives having carbazole as a core unit act as a push-pull chromophore, in which carbazole acts as a donor and opposite end of the styryl unit acts as an acceptor. Such push pull units have prime role as a basic building block in the second-order NLO chromophores [15]. They have enhanced two photon absorption and fluorescence quantum yield, hence they have been evaluated as two photon absorbing materials [16]. Several carbazole derivatives having styryl units at the third position have been designed and synthesized [17–21]. These mono styryl derivatives are reported to act as potential photobleaching data storage materials and they find use in the fabrication of two-photon microscopy devices for biological imaging [22, 23]. Their applicability covers the current emerging areas like electroluminescent materials, organic light emitting diodes [24, 25] and dye sensitized solar cells [26].

A carbazole derivative with methoxy substitution is of great importance in linking potential mesogenic NLO-carbazole system to the polysiloxane backbone; also it enhances the solubility of the monomer derived from carbazole [27]. We have synthesized the carbazole based styryl derivative having styryl group at the third position and a methoxy substitution at the fourth position. Further, we have evaluated the photophysical properties of the synthesized novel chromophores and calculated the ratio of the ground state to the excited state dipole moment. Density functional theory computations [B3LYP/6-31G(d)] were carried out to study the geometrical and electronic properties of the synthesized molecules.

Electronic supplementary material The online version of this article (doi:10.1007/s10895-014-1389-9) contains supplementary material, which is available to authorized users.

P. G. Umape · Y. Gawale · N. Sekar (✉)
Tinctorial Chemistry Group, Department of Dyestuff Technology, Institute of Chemical Technology (Formerly UDCT), Nathalal Parekh Marg, Matunga, Mumbai 400 019, India
e-mail: n.sekar@ictmumbai.edu.in

Experimental Section

Materials and Equipments

All the commercial reagents and solvents were procured from s.d. fine chemicals (India). The reaction was monitored by TLC using 0.25 mm E-Merck silica gel 60 F_{254} precoated plates, which were visualized with UV light. Melting points were measured on standard melting point apparatus from Sunder industrial product Mumbai, and are uncorrected. The FT-IR spectra were recorded on a JASCO 4100 FT-IR Spectrometer. ^{1}H NMR spectra were recorded on VXR 300 MHz and Bruker 500 MHz instruments using TMS as an internal standard. The visible absorption spectra of the compounds were recorded on a Spectronic Genesys 2 UV-Visible spectrophotometer. Fluorescence spectra of the compounds are recorded on Varian Cary Eclipse Spectrofluorimeter.

Synthesis and Characterization

Synthesis of 4-Methoxy-9-Methyl-9H-Carbazole-3-Carbaldehyde 3

Sodium hydride 60 % (5.45 g, 136.45 mmol) was taken in 30 ml of dry THF and cooled to 0 °C under nitrogen atmosphere. 9H-Carbazole-4-ol (10 g, 54.64 mmol) was slowly added in 30 ml THF and allowed to dissolve by maintaining the temperature of reaction mass at 0 °C. The mixture was stirred for 30 min and then methyl iodide (8.70 ml, 136.45 mmol) was added. The reaction mass was then brought to room temperature and stirred for 2 h under nitrogen atmosphere. The progress of the reaction was monitored on TLC. On completion of the reaction the unreacted excess of sodium hydride was quenched by adding t-butyl alcohol under the cooling condition. The solvent THF was distilled out and cold water was added to the residual mass, stirred well and filtered. This crude methylated product (10 g, 47.00 mmol) **2** dissolved in 20 ml DMF and was added drop wise into the stirred solution of phosphorus oxychloride (4.9 ml, 52.00 mmol) in DMF (17.0 ml, 219.53 mmol) within 30 min maintaining the temperature between 0 and 5 °C, reaction mass allowed to stirred for 30 min maintaining the temperature 0–5 °C. The mixture was then brought to room temperature and then heated at 70–75 °C for 1 h. The progress of the reation was monitored by TLC, and TLC showed the formation of two products. The reaction was cooled down, stirred well and neutrilised with sodium bicarbonate. The precipitated product was filtered and dried. The crude product was found to be a mixture of 4-methoxy-9-methyl-9H-carbazole-3-carbaldehyde **3** and 4-methoxy-9-methyl-9H-carbazole-1-carbaldehyde 4. The compound **3** and **4** were separated by column chromatography on silica 100–200 mesh using toluene as eluent.

Yield=48 %; Melting point=120–122 °C

FT-IR=1,662 cm^{-1} (C=O), 1,589 cm^{-1} (C=C, aromatic),

^{1}H NMR ($CDCl_3$, 300 MHz)=δ 10.50 (s, 1H), δ 8.27 (d, 1H, *J*=8.4 Hz), δ 8.01 (d, 1H, *J*=8.4 Hz), δ 7.55 (t, 1H, *J*=7.7, 7.3 Hz), δ 7.46 (d,1H, *J*=7.7 Hz), δ 7.36 (t, 1H, *J*=8.0, 7.7 Hz) δ 7.25 (d, 1H, *J*=8.0 Hz), δ 4.19 (s, 3H), δ 3.90 (s, 3H).

Synthesis of (E)-2-(Benzo[d]Thiazol-2-yl) -3-(4-Methoxy-9-Methyl-9H-Carbazol-3-yl)Acrylonitrile **6a**

A mixture of 4-methoxy-9-methyl-*9H*-carbazole-3-carbaldehyde **3** (0.50 g, 2.09 mmol) and 2-cyanomethyl-1,3-benzothiazole (0.36 g, 2.09 mmol) was stirred in ethanol(10 ml). The solution was refluxed for 2 h with a catalytic amount of piperidine. The progress of the reaction was monitored on TLC. The yellow solid separated was filtered and dried. The crude product was purified by column chromatography using silica of mesh size 100–200 using toluene as the eluent.

Yield=66 %; Melting point=260–262 °C.

FT-IR=2,209 cm^{-1} (CN), 1,664 cm^{-1} (C=C, olefinic) 1,560 cm^{-1} (C=C, aromatic)

Mass=*m/z* 396 (M+1).

^{1}H NMR ($CDCl_3$, 300 MHz)=δ 8.77 (s, 1H), δ 8.66 (d, 1H, *J*=9 Hz), δ 8.27 (d, 1H, *J*=7.8 Hz), δ 8.11 (d, 1H, *J*=8.1 Hz), δ 7.90 (d, 1H, *J*=7.8 Hz), δ 7.58–7.34 (m, 5H), δ 7.32 (d, 1H, *J*=8.7 Hz), δ 4.15 (s, 3H), δ 3.91 (s, 3H).

Synthesis of (E)-2-(1H-Benzo[d]imidazol-2-yl) -3-(4-Methoxy-9-Methyl-9H-Carbazol-3-yl)Acrylonitrile **6b**

A mixture of 4-methoxy-9-methyl-*9H*-carbazole-3-carbaldehyde **3** (0.50 g, 2.09 mmol) and 2-(cyano methyl)benzimidazole (0.33 g, 2.09 mmol) was stirred in ethanol(10 ml). The reaction mixture was refluxed for 2 h with a catalytic amount of piperidine. The progress of the reaction was monitored on TLC. The yellow solid separated was filtered and dried. The crude product **6b** was purified by column chromatography using silica of mesh size 100–200, the column was carried out starting with toluene and further ethyl acetate was added from 1 to 10 %.

Yield=57 %; Melting point=265–270 °C.

FT-IR=2,923 cm^{-1} (NH), 2,221 cm^{-1} (CN), 1,600 cm^{-1} (C=C, olefinic) 1,528 cm^{-1} (C=C, aromatic).

Mass=*m/z* 379 (M+1).

^{1}H NMR ($CDCl_3$, 500 MHz)=δ 9.04 (s, 1H), δ 8.41 (d, 1H, *J*=7 Hz), δ 8.09 (d, 1H, *J*=7.5 Hz), δ 7.73 (bp, 3H), δ 7.52 (t, 2H, *J*=7.5, 7.5 Hz), δ 7.36–7.30 (m, 2H), δ 7.06 (d, 1H, *J*=8.5 Hz), δ 5.3 (s, 1H), δ 4.14 (s, 3H), δ 3.91 (S, 3H).

Synthesis of (Z)-3-(4-Methoxy-9-Methyl-9H-Carbazol-3-yl) -2-(4-Nitrophenyl) Acrylo-Nitrile **6c**

A mixture of 4-methoxy-9-methyl-9*H*-carbazole-3-carbaldehyde **3** (0.50 g, 2.09 mmol) and *p*-nitro benzyl cyanide (0.36 g, 2.09 mmol) was stirred in 10 ml ethanol. The reaction mixture was refluxed for 2 h with a catalytic amount of piperidine. The progress of the reaction was monitored on TLC. The orange solid separated was filtered and dried. The crude product **6c** was purified by column chromatography using silica of mesh size 100–200 using toluene as the eluent.

Yield=61 %; Melting point=228–230 °C

FT-IR=2,210 cm^{-1} (CN), 1,625 cm^{-1} (C=C, olefinic), 1,595 cm^{-1} (C=C, aromatic),

1,550 cm^{-1} (NO_2).

Mass=*m/z* 384 (M+1).

^{1}H NMR ($CDCl_3$, 300 MHz)=δ 8.59 (d, 1H, *J*=8.7 Hz), δ 8.32 (t, 3H, *J*=9 Hz), δ 8.26 (d, 1H, *J*=8.1 Hz), δ 7.90 (d, 2H, *J*=9 Hz), δ 7.56 (t, 1H, *J*=8.7, 7.2 Hz), δ 7.48 (d, 1H), δ 7.34–7.39 (m, 2H), δ 4.10 (s, 3H), δ 3.92 (s, 3H).

Computational Details

The ground state geometry of the compounds **6a**–**6c** in their C_s symmetry were optimized using the tight criteria in vacuum and in polar (DMF, ethanol, methanol, acetonitrile, and acetone) and non-polar (ethylacetate, chloroform, dichloromethane, and THF) solvents using density functional theory [28] and Polarizable Continuum Model (PCM). The functional used in this study was B3LYP. The B3LYP method combines Becke's three parameter exchange functional (B3) [29] with the nonlocal correlation functional by Lee, Yang, and Parr (LYP) [30–33]. The basis set used for all atoms was 6-31G(d) [34–36]. The vertical excitation energies at the ground-state equilibrium geometries were calculated with TD-DFT [37, 38]. The low-lying first singlet excited state (S_1) of each tautomer was relaxed using the TD-DFT to obtain its minimum energy geometry. The difference between the energies of the optimized geometries in the first singlet excited state and the ground state was used in computing the emissions [39–43]. All electronic structure computations were carried out using the Gaussian 09 program [44].

Results and Discussion

Chemistry

Synthesis and Characterization of Synthesized Styryl Dyes **6a**–**6c.**

Knoevenagel condensation between 4-methoxy-9-methyl-9*H*-carbazole-3-carbaldehyde **3** and different active methylene derivatives (**5a**–**5c**) were carried out in order to synthesize the styryl derivatives **6a**–**6c** having carbazole as a core structure with styryl unit at the third position. 2-Cyanomethyl-1,3-benzthiazole **5a**, 2-(cyanomethyl)benzimidazole **5b** and *p*-nitro benzyl cyanide **5c** were used as active methylene compounds.

4-Hydroxy carbazole **1** was reacted with methyl iodide to yield 4-methoxy-9-methyl-9*H*-carbazole **2**. The 4-methoxy-9-methyl-9*H*-carbazole **2** on Vilsmeier formylation gives a mixture of 4-methoxy-9-methyl-9*H*-carbazole-3-carbaldehyde **3** and 4-methoxy-9-methyl-9*H*-carbazole-1-carbaldehyde **4**. Further, 4-methoxy-9-methyl-9*H*-carbazole-3-carbaldehyde **3** was isolated by purification and subjected to Knoevenagel condensation with the different active methylene moieties mentioned above to produce the targeted styryl derivatives **6a**–**6c** (Scheme 1 and Fig. 1)

Photophysical properties of the dyes **6a**–**6c** were investigated and also the ratio of the ground state dipole moment to the excited state dipole moment was calculated using solvatochromism method.

Photophysical Properties of Styryl Dyes **6a**–**6c**

The dyes are bright yellow to orange in color. The dye **6a** has strong yellow fluorescence in solid state (emission 558 nm, exCitation 416) and the dye **6c** has strong orange fluorescence in solid state (emission 606 nm, exCitation 413), while the dye **6b** does not show solid state fluorescence Figs. 2, and 3. The photograph of the sample under UV-light and the solid state excitation and emission are in SI (Fig. 1 and Table 1).

The synthesized styryl derivatives absorb in range of 392 to 425 nm and emission was observed between 429 and 593 nm. The Stokes shifts of these molecules lies in between 34 and 174 nm. Figure 4 represents absorption spectra of the dyes **6a**–**6c** in dichloromethane, and from this it is clear that the dye **6a** with benzthiazole substitution and the dye **6c** with *p*-nitro benzyl substitution absorbs near about same wavelength with almost equal intensity. Dye **6b** with benzimidazole substitution absorbs at shorter wavelength than the dye **6a**, and hence we can say that replacing benzimidazole unit with benzthiazole unit leads to a bathochromic shift in the styryl chromophore. The corresponding emissions of these dyes in dichloromethane are shown in Fig. 8. It is seen that the dye **6a** which has benzimidazole at acceptor end emits with excellent fluorescent intensity around 12 times more intense. If we compare the emission wavelengths *p*-nitro benzyl substituted dye **6c** has a red shifted emission and the dye **6b** blue shifted emission as compared to the dye **6a**.

The synthesized dyes **6a**–**6c** are of push-pull type and such chromophores exhibit the intramolecular charge transfer phenomenon. The intramolecular charge transfer phenomenon between acceptor and donor terminal greatly affects the photophysical properties of fluorescent molecules. This is well agreement with HOMO-LUMO of the synthesized molecules. This is also governed by number of factors. Out of

Scheme 1 Synthesis of styryl dyes from 4-methoxy-9-methyl-9*H*-carbazole-3-carbaldehyde **6a–6c**

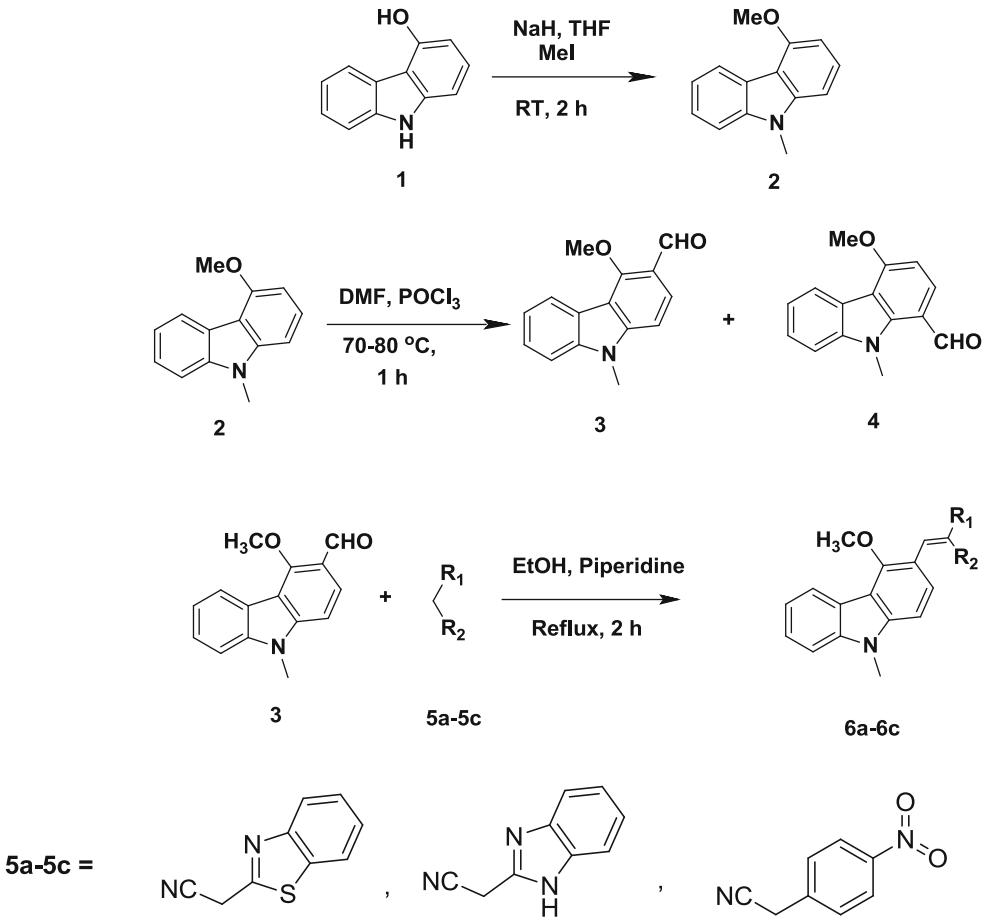

these, polarity of solvent is one of the crucial parameter. Polarity of solvent affects directly to photophysical properties of chromophores. Hence, in this section we have studied solvatochromic and solvatofluoric characteristics of synthesized dyes **6a**–**6c**.

Effect of Solvent Polarities on Absorption Properties

The styryl colorants synthesized can be considered as donor-π-acceptor (D-π-A) molecules. The carbazole ring acts as the electron donating unit, while the benzthiazole, benzimidazole, and *p*-nitro benzyl substituents act as the electron

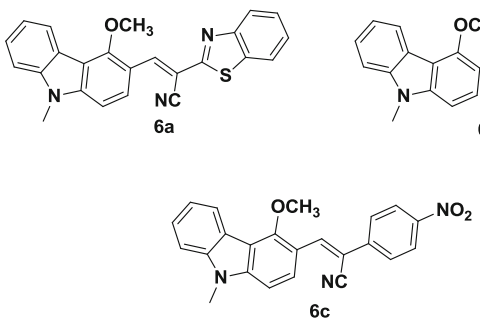

Fig. 1 Structures of the synthesized dyes **6a–6c**

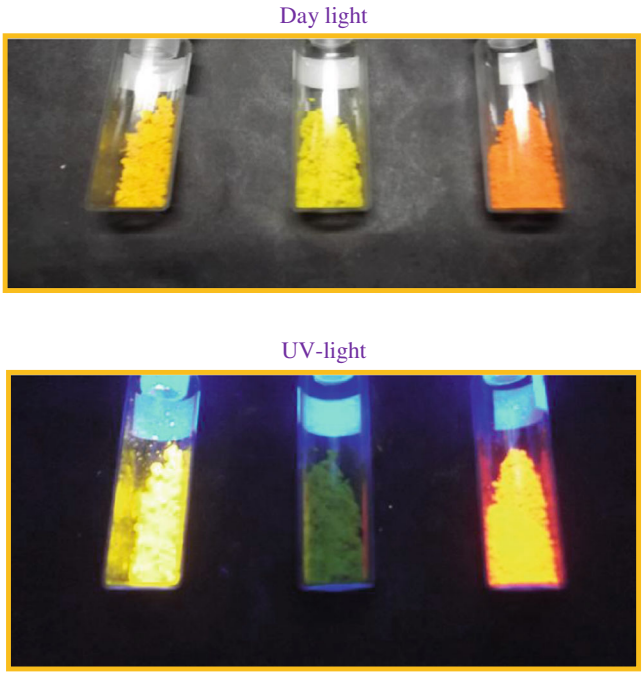

Fig. 2 Photographs of dyes **6a–6c** in day light and UV-light to show solid state fluorescence

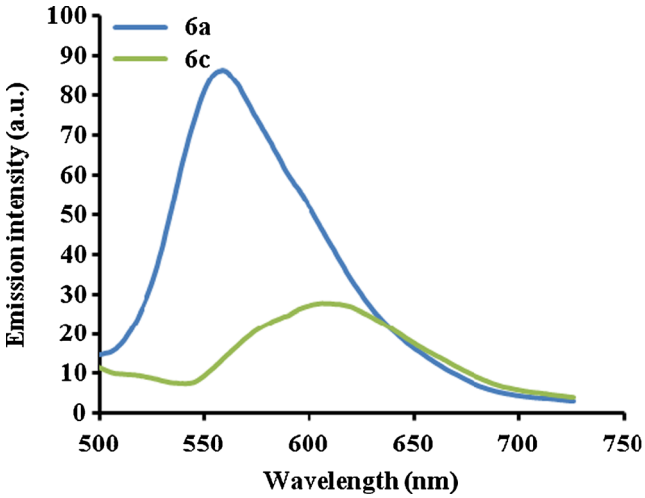

Fig. 3 Overlay Solid state fluorescence spectra of comp **6a** and **6c**

withdrawing units conjugated through the olefinic bond. The styryl molecules **6a**–**6c** absorb in the range 392–422 nm. The dye **6a** has a blue shifted absorption compared to the dye **6b** indicating that the benzothiazolyl ring is a better acceptor than the benzimidazolyl ring. These experimental results are supported by TD-DFT and the results are in good agreement (Table 6–8) with the computed values. The dye **6a** shows blue shifted absorption in ethyl acetate (416 nm) and red-sifted absorption in MeOH (422 nm). Similar results were obtained theoretically in ethyl acetate (431 nm) and in MeOH (435 nm). In the case of the compounds 6a, 6b and 6c the experimental absorption maxima are close to the vertical excitation data obtained from TD-DFT computations. The emission maxima of the synthesized molecules were in the range 430–593 nm. The absorption spectra of the dye **6a** in different solvents of increasing polarity do not show any abrupt change in the absorption wavelength (Table 8). But it has been observed that **6a** has the maximum absorption intensity in dichloromethane, while in acetonitrile it absorbs with the lowest absorption intensity (Fig. 5). In the case of the compound **6b** maximum absorption intensity has been observed in ethyl acetate, while in methanol it absorbs with the lowest absorption intensity. And in the case of the compound **6c** the maximum absorption intensity has been seen in acetonitrile, while in THF it absorbs with the lowest absorption intensity. There is a slight red shift observed in ethanol and DMF with the absorptions at 422 and 425 nm respectively. In the case of the compound **6b**, blue shift is observed in ethanol chloroform and DCM (Table 7) and **6c** has shown blue

Table 1 Solid state fluorescence data of comp **6a** and **6c**

Dye	Abs. λmax (nm)	Emis. (nm)	Emis. intensity
6a	416	558	86.21
6c	413	606	27.75

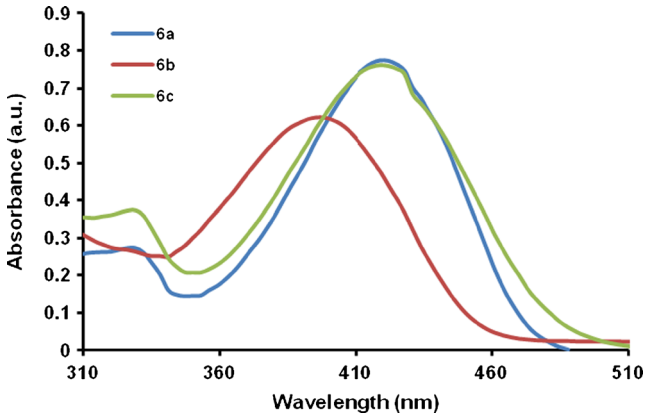

Fig. 4 Absorption spectra of dyes **6a**–**6c** in dichloromethane

shift in chloroform, DCM and THF (compared to the other solvents studied) (Table 8).

Effect of Solvent Polarity on Fluorescence Emission

The effect of solvent polarity on the fluorescence properties of the styryl dyes was studied. The compound **6a** showed blue shift with the increase in the solvent polarity. It emits at 484 nm in ethyl acetate and at 487 nm in acetonitrile. Stokes shift decreases in the order with increase in solvent polarity (Table 2). The overlay of emission spectra clearly indicates that the emission intensity of the compound **6a** is good in chloroform, dichloromethane, ethyl acetate, and acetone, while in EtOH, DMF and acetonitrile it has the emission intensity below 0.5 a.u. (Fig. 5). The compound 6b emits at around 481 nm in most of the listed solvents, but it has red shifted emission in DMF (488 nm) and a blue shifted emission in THF (429 nm).

Solvatochromism and Solvatofluorism

The solvatochromism and solvatofluorism studies of the synthesized dyes **6a**–**6c** were carried out at the concentration 1×

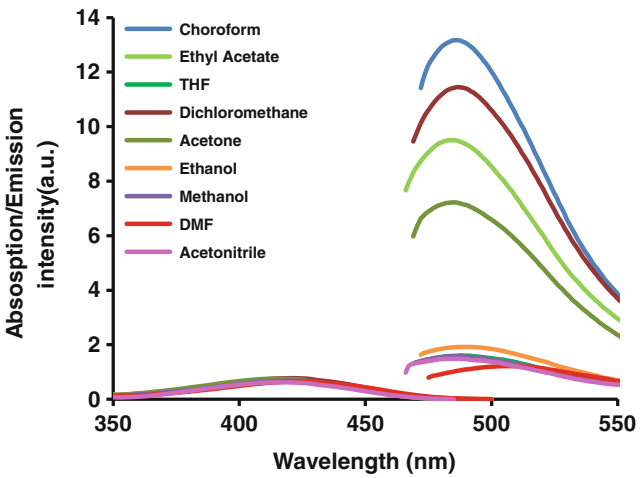

Fig. 5 Absorption/emission spectra of dye **6a** in different solvents

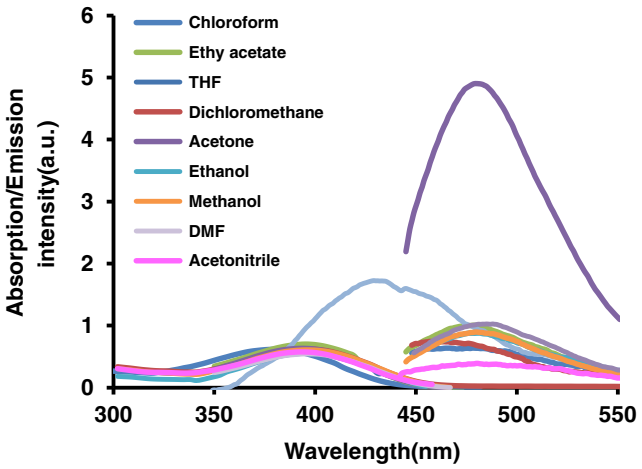

Fig. 6 Absorption/emission spectra of dye **6b** in different solvents

10^{-6} mol L^{-1} in different solvents of varying polarity. The results obtained are summarized in Tables 2, 3, and 4 and the overlay spectra of each compound in different solvents are presented in Fig. 5, 6, and 7.

The dye **6a** (Table 2) absorbs at 419 nm in most of the solvents. While bathochromic shift of 6 nm was observed in DMF (425 nm), also in chloroform and ethanol it shows the absorption at 422 nm. Overlay absorption spectra of the dye **6a** in different solvents is shown in Fig. 5, which indicates that a strong absorption occurs in dichloromethane and a weak absorption in acetonitrile. From Table 3, it can be concluded that the dye **6b** absorbs either at 395 or 398 nm in different solvents. A blue shift in the absorption (at 392 nm) is seen only in acetonitrile, its overlay absorption spectra shows strong absorption characteristics of this dye in ethyl acetate and weaker absorption pattern in ethanol (Fig. 6). The dye **6c** shows absorption maxima at 419 or 413 nm in majority of the solvents, while in ethanol the absorption was observed at 416 nm (Table 4). The absorption pattern in different solvents is presented in Fig. 7 which indicates its absorption pattern with weaker absorption in THF while in acetonitrile it shows strong absorption than in the other solvents.

The emission characteristics of these dyes **6a**–**6c** were also studied and the results obtained are summarized in Tables 2, 3, and 4. Figures 5, 6, and 7 represent the emission overlay spectra of the dyes **6a**–**6c**. The solvatofluorism study of the dye **6a** in different solvents is summarized in Table 2. The emission of this dye in majority of the solvents lie in the range 484–490 nm but in DMF a bathochromic shift is observed at 505 nm. Here, the emission pattern shown in Fig. 5 clearly indicates that appreciable emissive properties are observed in the following solvents in the decreasing order of intensity, chloroform>dichloromethane>ethyl acetate>acetone. For the remaining solvents, the emission intensity lies below 2 a.u., the dye **6a** emits with the lowest intensity in DMF. In the case of the dye **6b**, the emission maxima in polar solvents such as acetone, ethanol, methanol and acetonitrile are observed at 480–481 nm, and in DMF it has the longest emission wavelength at 488 nm amongst all the solvents used. The emission at the shortest wavelength is observed in THF at 429 nm (Table 3). The emission overlay spectra of the dye **6b** shows substantial emission intensity in acetone, and in acetonitrile the emission is with the lowest emission intensity (Fig. 6).

Solvatofluorism study of the dye **6c** illustrates that the emission range in most of the solvents is 536–548 nm. The red shifted emission is observed in dichloromethane at 593 nm, while blue shift in the emission maxima is observed in chloroform at 481 nm. The emission intensity in chloroform is found to be the strongest one, while in acetonitrile very weak emission was observed (Fig. 7).

Out of these chromophores, the dye **6c** emits with the largest Stokes shift of 174 nm in dichloromethane and the shortest Stokes shift observed was 62 nm (Table 4). The Stokes shifts obtained for the dye **6a** ranges between 64 and

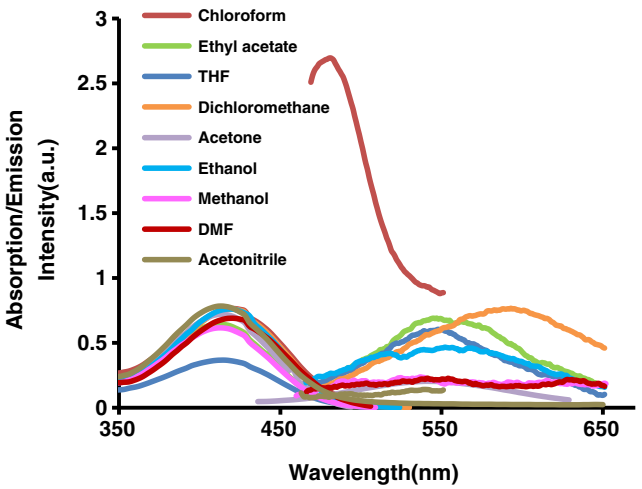

Fig. 7 Absorption/emission spectra of dye **6c** in different solvents

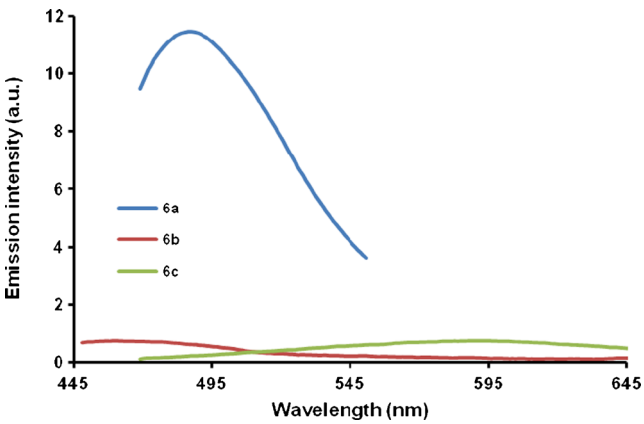

Fig. 8 Emission spectra of dyes **6a**–**6c** in dichloromethane

Table 2 Photo-physical properties of the dye **6a** in different solvents

Solvents	Dye **6a**						
	λ_{abs}^{max} [a] (nm)	λ_{ems}^{max} [b] (nm)	λ_{exct}^{max} [c] (nm)	Stokes shift (nm)	Stokes shift (cm^{-1})	[E] ($lit.mole^{-1}$ cm^{-1})	Φ_f [d]
Chloroform	422	486	422	64	3120.551	28,276	0.0288
Ethyl acetate	416	484	418	68	3377.305	26,220	0.0240
THF	419	488	417	69	3374.545	27,485	0.0143
Dichloromethane	419	486	420	67	3290.217	30,609	0.0511
Acetone	419	485	417	66	3247.792	29,977	0.0298
Ethanol	422	490	420	68	3288.519	25,587	0.0052
Methanol	419	485	416	66	3247.792	26,891	0.0049
DMF	425	505	429	80	3727.432	26,061	0.0040
Acetonitrile	416	487	418	71	3504.581	24,677	0.0080

[a] Absorption wavelength maxima

[b] Fluorescence emission maxima

[c] Fluorescence excitation maxima

[d] Fluorescence quantum yield

THF Tetrahydrofuran; *DMF N,N* Dimethylformamide

69 nm, while in DMF and in acetonitrile a larger Stokes shift of 80 and 71 nm is observed (Table 2). The dye **6b** has the largest Stokes shift of 93 nm in DMF, and in THF the smallest Stokes shift of 34 nm is observed. In chloroform and dichloromethane, the dye has an emission with Stokes shifts of 69 and 61 nm, while in the other solvents the Stokes shifts are observed from 83 to 88 nm (Table 3). The excitation maxima for the dye **6a** are nearly the same as the absorption maxima (Table 2). For the dye **6b** in chloroform, dichloromethane and acetonitrile the absorption maxima and excitation maxima are of nearly same value. For other solvents excitation occurs at a higher wavelength, but in THF excitation occurs at lower wavelength (Table 3). The excitation of the dye **6c** in all the solvents occurs at higher wavelengths than the absorption wavelengths and the excitation rage is 428 nm to 450 nm (Table 4 and Fig. 8).

Quantum Yield

The quantum yield of the compounds **6a**–**6c** was calculated by the known procedure [45]. In order to calculate quantum yield of the synthesized fluorescent styryl dyes **6a**–**6c** fluorescein is chosen as the reference standard. Quantum yields of these dyes **6a**–**6c** are calculated in different solvents of different polarities and the obtained values are summarized in Tables 2, 3, and 4. From Table 2, higher values of quantum yields are observed in non-polar solvents, the dye **6a** emits with the highest quantum efficiency of 0.0511 in dichloromethane. In

Table 3 Photo-physical properties of the dye **6b** in different solvents

Solvents	Dye **6b**						
	λ_{abs}^{max} (nm)	λ_{ems}^{max} (nm)	λ_{exct}^{max} (nm)	Stokes shift (nm)	Stokes shift (cm^{-1})	[E] ($lit.mole^{-1}$ cm^{-1})	Φ_f
Chloroform	398	467	395	69	3712.352	23,348	0.0102
Ethyl acetate	395	479	417	84	4439.629	26,527	0.0121
THF	395	429	368	34	2006.432	21,116	0.0340
Dichloromethane	398	459	398	61	3339.136	23,500	0.1494
Acetone	395	480	424	85	4483.122	23,916	0.0168
Ethanol	398	481	423	83	4335.607	20,964	0.0021
Methanol	395	480	427	85	4483.122	23,121	0.0020
DMF	395	488	428	93	4824.652	20,548	0.0025
Acetonitrile	392	480	390	88	4676.871	21,797	0.0031

Table 4 Photo-physical properties of the dye **6c** in different solvents

Solvents	Dye **6c**						
	λ_{abs}^{max} (nm)	λ_{ems}^{max} (nm)	λ_{exct}^{max} (nm)	Stokes shift (nm)	Stokes shift (cm^{-1})	^{E} (lit.$mole^{-1}$ cm^{-1})	Φ_f
Chloroform	419	481	428	62	23866.35	29,298	0.0376
Ethyl acetate	413	547	432	134	24213.08	24,690	0.0018
THF	413	548	430	135	24213.08	14,054	0.0346
Dichloromethane	419	593	439	174	23866.35	29,183	0.0104
Acetone	413	540	439	127	24213.08	27,609	0.0005
Ethanol	416	552	451	136	24038.46	29,183	0.0009
Methanol	413	536	438	123	24213.08	23,615	0.0013
DMF	419	541	450	122	23866.35	26,457	0.0011
Acetonitrile	413	540	439	127	24213.08	30,066	0.0005

the polar solvents, quantum efficiency values are low and the lowest value is observed in DMF (0.0040). Similarly, for the dye **6b** quantum yield values are tabulated in Table 3 which clearly indicates the enhanced quantum efficiency in non-polar solvent and the lower values of quantum efficiency in polar solvents. In dichloromethane significant value of the quantum yield (0.1494) is observed and in methanol it goes down to the lowest value of 0.0025. Quantum yields of the dye **6c** show that a higher values of quantum yields are obtained in chloroform and THF, while in the other solvents quantum efficiencies are lower (Table 4).

Determination of Dipole Moment by Solvatochromic Method

5The push-pull type of chromophores undergoes intramolecular charge transfer phenomenon [46]. This charge transfer phenomenon leads to the molecular polarization, as well as photophysical properties of molecules are also directly dependent upon the extent of intramolecular charge transfer phenomenon [47]. As photophysical properties of the fluorescent molecules are greatly affected by the solvent parameters such as polarity, permittivity, viscosity, refractive index etc., the ground state and excited state dipole moments of the molecules also altered by solvent parameters. Based on these above assumptions Bakhshiev [48] and Kawski-Chamma-Viallet [49, 50] derived equations relating the solvent parameters with the ground and the excited state dipole moments. This method gives a linear correlation between the absorption and the emission wavelengths in cm^{-1} and the solvent polarity functions [51–53] obtained by Bakhshiev and Kawski-Chamma-Viallet. Here we have used these models to calculate the ratio of the excited state dipole moment to the ground state dipole moment of the synthesized dyes. The theoretical dipole moment calculations are described in Supporting information (SI) The results of theoretical dipole moment are summarized in Table 5. From the Table 5, it is obvious that the dipole moments of the dyes **6a**–**6c** in ground state are more polarized than the dipole moments in excited state. For the dye **6a**, ground state dipole moment is almost double the excited state. The dipole moment ratio of the dye **6c** indicates that it is highly polarized in the ground state than the excited state. The dipole moments of compounds obtained by computationally in different solvents are summarized in SI Table 3, 4, and 5.

Computational Study

Density Functional Theory [B3LYP/6-31G(d)] computations have been used to understand structural, molecular, electronic and photophysical parameters of the synthesized carbazole based styryl dyes. The experimental photophysical properties like absorption and emission of the dyes **6a**–**6c** were correlated with the computed vertical excitation and the results are summarized in Tables. 6, 7, and 8. The % deviation between experimental absorption wavelengths and vertical excitation of the compound **6a** is approximately 3 % in all solvents studied. In the case of compounds **6b** and **6c**, significant difference was observed between the experimental wavelength and the vertical excitation in polar as well as nonpolar solvents. The % deviation is large (11 %) in DCM for the compound **6b**, while in other solvents it is in the range between 5 and 7 %. In the case of the compound **6c**, the % deviation is in the range between 15 and 18 and it is

Table 5 Excited state and ground state dipole moment (in Debye) ratio value for dyes **6a**–**6c**

Dye	$\lvert m_1+m_2 \rvert$	$\lvert m_1-m_2 \rvert$	$\frac{\mu_e}{\mu_g}$
6a	859	1,713	0.50
6b	371	5,143	0.07
6c	0.1	4,139	0.00

Table 6 Observed UV-visible absorption and computed absorption of compound **6a** in different solvents

Solvents	TD-DFT								
	λmax expt.nm	Vertical excitation			*F*	A major contribution	Observed emission	TD-DFT emission	% D
		nm	eV	% D					
CHCl3	422	432	2.8656	2.36	1.188	H→L (99 %)	486	432	11.1
EtOAc	416	431	2.870	3.6	1.202	H→L (99 %)	484	475	1.8
THF	419	433	2.859	3.3	1.211	H→L (99 %)	488	478	2.0
DCM	419	434	2.851	3.5	1.216	H→L (99 %)	486	480	1.2
Acetone	419	432	2.851	3.1	1.186	H→L (99 %)	485	487	0.4
EtOH	422	435	2.849	3.1	1.186	H→L (99 %)	490	488	0.4
MeOH	419	435	2.854	3.8	1.172	H→L (99 %)	485	489	0.8
DMF	425	437	2.835	2.8	1.147	H→L (99 %)	505	436	13.6
ACN	416	434	2.8506	4.3	1.1783	H→L (99 %)	487	490	0.6

comparatively large as compared to the compounds 6a and **6b**. The major contribution from the ground state to the excited state in all the solvents is observed from HOMO to LUMO+1 (99 %) with a high oscillator strength.

The carbazole based styryl dyes **6a**–**6c** show the emission maxima in the visible region. The compound 6c shows a red shifted emission as compared to the compounds **6a** and **6b**. TD-DFT computation was performed to support the experimental emission. The experimental emissions of the compounds **6a**–**6c** in solvents of different polarity were compared with the computed values (Tables. 6, 7, and 8), the experimental emission and the computed emission values are close to each other for the compounds **6a**–**6c**, except in $CHCl_3$ and DMF for the compound **6a**, in THF for the compound **6b** and in DCM for the compound **6c**. The difference between the experimental emission and the computed emission is almost the same in the polar solvents (methanol, ethanol, and DMF) and the nonpolar solvents (acetonitrile, DCM, chloroform, ethyl acetate, acetone and THF).

The HOMO and LUMO diagrams for the compounds **6a**–**6c** are shown in Fig. 9. In acetone solvent. In the case of the compound **6a** electron density is concentrated on the thiazole ring in HOMO and the node on the cyanide and the π system, while in the case of LUMO the electron density is located on the cyanide and the π system and the nodes on the thiazole units. In the case of the compound **6b** the electron density is distributed over the entire molecule for HOMO and in LUMO the electron density on the benzimidazole and on the cyanide and the π system which indicates that in the compound 6b the electron flow is from the donor carbazole to the acceptor benzimidazole units through the π-bridge. In the case of the compound **6c** in HOMO the electron density is on the carbazole unit and the nodes on the acceptor unit, but in the case of LUMO the electon density is on the acceptor units. The

Table 7 Observed UV-visible absorption and computed absorption of compound **6b** in different solvents

Solvent	λmax expt. nm	TD-DFT							
		Vertical excitation			*f*	A major contribution	Observed emission	TD-DFT emission	% D
		nm	eV	% D					
CHCl3	398	425	2.917	6.7	1.238	H→L (99 %)	467	468	1.7
EtOAc	395	423	2.926	7.0	1.214	H→L (99 %)	479	471	1.6
THF	395	424	2.917	7.3	1.224	H→L (99 %)	429	473	10.0
DCM	398	445	2.912	11.0	1.229	H→L (99 %)	459	475	3.4
Acetone	395	424	2.917	7.3	1.205	H→L (99 %)	480	480	0
EtOH	398	425	2.916	6.7	1.205	H→L (99 %)	481	481	0
MeOH	395	424	2.921	7.3	1.193	H→L (99 %)	480	482	0.4
DMF	395	426	2.9053	7.8	1.200	H→L (99 %)	488	426	12.7
ACN	392	424	2.918	8.1	1.194	H→L (99 %)	480	482	0.4

Table 8 Observed UV-visible absorption and computed absorption of compound **6c** in different olvents

Solvent	λmax expt. nm	TD-DFT							
		Vertical excitation			*f*	A major contribution	Observed emission	TD-DFT emission	% D
		Nm	eV	% D					
CHCl3	419	478	2.5919	14.00	0.7758	H→L(99 %)	481	507	5.4
EtOAc	413	479	2.5848	15.98	0.7464	H→L(99 %)	547	540	1.2
THF	413	482	2.5697	16.70	0.7511	H→L(99 %)	548	529	3.4
DCM	419	484	2.5595	15.51	0.7530	H→L(99 %)	593	531	10.5
Acetone	413	487	2.5440	17.91	0.7225	H→L(99 %)	540	538	0.3
EtOH	416	488	2.5406	17.30	0.7218	H→L(99 %)	552	540	2.1
MeOH	413	487	2.5410	17.91	0.7098	H→L(99 %)	536	541	0.9
DMF	419	484	2.5571	15.51	0.7086	H→L(99 %)	541	483	10.7
ACN	416	488	2.5381	17.30	0.7145	H→L(99 %)	540	541	0.1

HOMO-LUMO energy gaps for the compounds **6a**–**6c** were computed by DFT. The compounds **6a**, **6b** and **6c** are not showing an effective solvatochromism and solvotoflurosium properties. The absorption and emission maxima of each compound in different solvents are almost same. These experimental results are supported by DFT. The energy gap between LUMO-HOMO of the compounds **6a**–**6c** is the same in all the solvents. The energy gap between HOMO and LUMO of each compound in all the solvents studied is summarized in SI Table 6, 7, and 8.

Conclusion

In conclusion, novel carbazole based styryl dyes **6a**–**6c** with the styryl unit at the 3rd position and a methoxy substitution are synthesized and characterized by FT-IR, ^{1}H NMR and Mass spectral analysis. A simple and efficient protocol was used for the synthesis of these dyes. These dyes are bright yellow to orange in color. The dye **6a** has a strong yellow fluorescence and the dye **6c** has a strong orange fluorescence in the solid state. The dye **6a** with the benzimidazole unit as

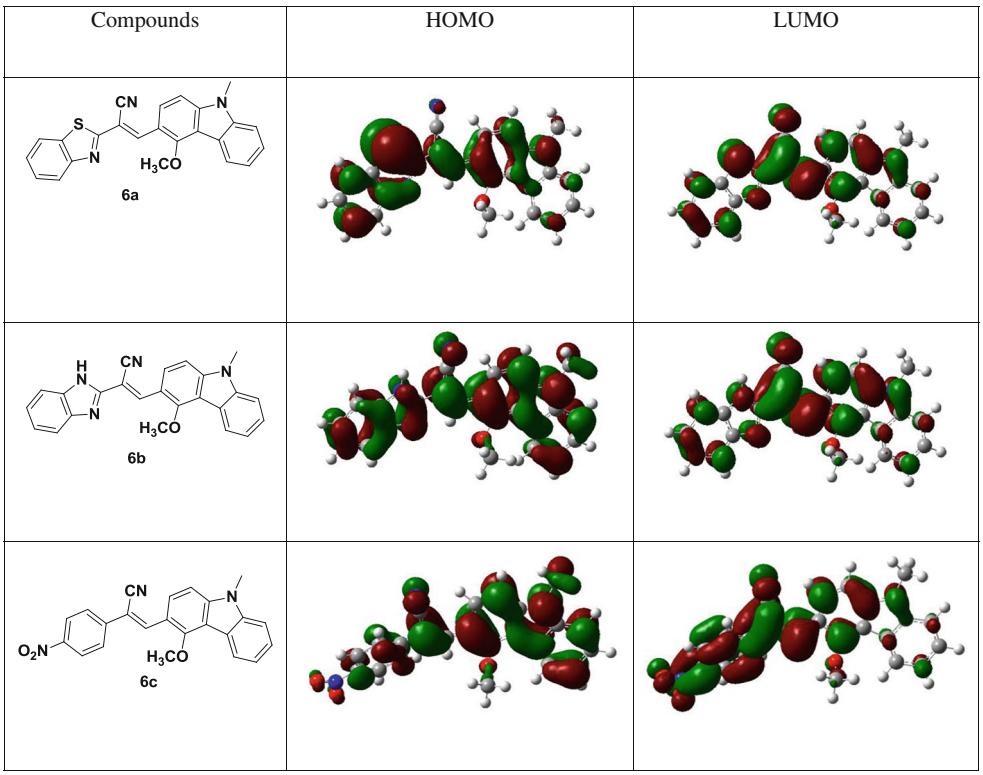

Fig. 9 HOMO-LUMO diagrams of compounds **6a**–**6c** in acetone solvent

the acceptor end group emits with excellent fluorescent intensity. Solvatofluorism study reveals that dye **6a** and **6b** emit with red shift in DMF and **6c** emits with a red shift in dichloromethane. The dye **6c** has a large Stokes shift in most of the solvents; in dichloromethane the largest Stokes shift of 174 nm is observed. The quantum yield of the dye **6b** has an appreciable value of 0.1494 in dichloromethane. The calculated ratios of the excited state dipole moment to the ground state dipole moment clearly indicate that the ground state is more polarized than the excited state for all the dyes **6a**–**6c**.

Acknowledgments The authors (Prashant Umape and Yogesh Gawale) are thankful to UGC for providing fellowship under UGC-SAP programme.

References

1. Tsai M-H, Ke T-H, Lin H-W, Chung-Chih W, Chiu S-F, Fang F-C, Liao Y-L, Wong K-T, Chen Y-H, Wu C-I (2009) Triphenylsilyl- and trityl-substituted carbazole-based host materials for blue electrophosphorescence. ACS Appl Mater Interfaces 1(3):567–574
2. Justin Thomas KR, Lin JT, Tao Y, Ko C (2001) Light-emitting carbazole derivatives: potential electroluminescent materials. J Am Chem Soc 123:9404–9411
3. Li Y, Ding J, Day M, Tao Y, Lu J, D'iorio M (2003) Novel stable blue-light-emitting oligofluorene networks immobilized by boronic acid anhydride linkages. Chem Mater 15:4936–4943
4. Li J, Li Q, Liu D (2011) Novel thieno-[3,4-b]-pyrazines cored dendrimers with carbazole dendrons: design, synthesis, and application in solution-processed red organic light-emitting diodes. Appl Mater Interfaces 3:2099–2107
5. Zhang Y, Wada T, Wang L, Sasabe H (1997) Amorphous conjugated carbazole trimers for photorefractive materials. Chem Mater 9:2798–2804
6. Boudreault PT, Wakim S, Blouin N, Simard M, Tessier C, Tao Y, Leclerc M (2007) Synthesis, characterization, and application of indolo[3,2-b]carbazole semiconductors. J Am Chem Soc 129: 9125–9136
7. Wang E, Hou L, Wang Z, Ma Z, Hellstrom S, Zhuang W, Zhang F, Inganas O, Andersson MR (2011) Side-chain architectures of 2,7-carbazole and quinoxaline-based polymers for efficient polymer solar cells. Macromolecules 44:2067–2073
8. Baldo MA, Lamansky S, Burrows PE, Thompson ME, Forrest SR (1999) Very high-efficiency green organic light-emitting devices based on electrophosphorescence. Appl Phys Lett 75:4–6
9. Lamansky S, Djurovich PI, Abdel-Razzaq F, Garon S, Murphy DL, Thompson ME (2002) Cyclometalated Ir complexes in polymer organic light-emitting devices. J Appl Phys 92:1570–1575
10. Iraqi A, Wataru I (2004) Preparation and properties of 2,7-linked N-alkyl-9H-carbazole main-chain polymers. Chem Mater 16:442–448
11. Ponnapati R, Felipe MJ, Muthalagu V, Puno K, Wolff B, Advincula R (2012) Conjugated polymer network films of poly(p-phenylene vinylene) with hole-transporting carbazole pendants: dual photoluminescence and electrochromic behavior. Appl Mater Interfaces 4:1211–1218
12. Gupta VD, Padalkar VS, Phatangare KR, Patil VS, Umape PG, Sekar N (2011) The synthesis and photo-physical properties of extended styryl fluorescent derivatives of N-ethyl carbazole. Dyes Pigments 88:378–384
13. Weber L, Halama J, Werner V, Hanke K, Bohling L, Chrostowska A, Dargelos A, Maciejczyk M, Raza A, Stammler H, Neumann B (2013) 1,3,2-benzodiazaboroles with 1,3-pentafluorophenyl and tetrafluoropyridyl substituents as building blocks in luminescent compounds. Eur J Inorg Chem 24:4268–4279
14. Takagi K, Takao H, Nakagawa T (2010) Synthesis and characterization of nitrogen-linked carbazole-containing fluorescent polymers. J Polym Sci Polym Chem 48:3729–3735
15. Zhang Y, Wada T, Sasabe H (1996) Synthesis and characterization of second-order nonlinear optical main-chain polyurethanes containing acceptor-substituted carbazole units. Macromol Chem Phys 197: 1877–1888
16. Li L, Wu Y, Zhou Q, He C (2012) Experimental and theoretical studies on the one-photon and two-photon properties of a series of carbazole derivatives containing styrene. J Phys Org Chem 25:362–372
17. Gupta VD, Padalkar VS, Phatangare KR, Patil VS, Umape PG, Sekar N (2011) The synthesis and photo-physical properties of extended styryl fluorescent derivatives of *N*-ethyl carbazole. Dyes Pigments 88(3):378–384
18. Mingzhu L, Zhu Y, Ma K, Cao L, Wang K (2012) Facile synthesis and photo-physical properties of cyano-substituted styryl derivatives based on carbazole/phenothiazine. Spectrochim Acta A Mol Biomol Spectrosc 95:128–134
19. Liang M, Zhong-Yuan Wang L, Zhang H-YH, Sun Z, Xue S (2011) New organic photosensitizers incorporating carbazole and dimethylarylamine moieties for dye-sensitized solar cells. Renew Energy 36(10):2711–2716
20. Kim D, Lee JK, Kang SO, Ko J (2007) Molecular engineering of organic dyes containing *N*-aryl carbazole moiety for solar cell. Tetrahedron 63(9):1913–1922
21. Grigoras M, Vacareanu L, Ivan T, Catargiu AM (2013) Photophysical properties of isoelectronic oligomers with vinylene, imine, azine and ethylene spacers bearing triphenylamine and carbazole end-groups. Dyes Pigments 98(1):71–81
22. Hu ZJ, Sun PP, Li L, Tian YP, Yang JX, Wu JY, Zhou HP, Tao LM, Wan CK, Li M, Chen GH, Tang HH, Tao XT, Jiang MH (2009) Two novel π-conjugated carbazole derivatives with blue two-photon-excited fluorescence. Chem Phys 355:91–98
23. Gao YH, Wu JY, Li YM (2009) A sulfur-terminal Zn(II) complex and its two-photon microscopy biological imaging application. J Am Chem Soc 131:5208–5213
24. Chen C, Lin JT, Yeh MP (2006) Stilbene like carbazole dimer-based electroluminescent materials. Tetrahedron 62:8564–8570
25. Zeng H, Wang G, Zeng G, Li J (2009) The synthesis, characterization and electroluminescent properties of zinc(II) complexes for single-layer organic light-emitting diodes. Dyes Pigments 83:155–161
26. Kajiyama S, Uemura Y, Miura H, Hara K, Koumura N (2012) Organic dyes with oligo-n-hexylthiophene for dye-sensitized solar cells: relation between chemical structure of donor and photovoltaic performance. Dyes Pigments 92:1250–1256
27. Diaz JL, Dobarro A, Vilacampa B, Velasco D (2001) Structure and optical properties of 2,3,7,9-polysubstituted carbazole derivatives. Experimental and theoretical studies. Chem Mater 13:2528–2536
28. Treutler O, Ahlrichs R (1995) Efficient molecular numerical integration schemes. J Chem Phys 102:346–354
29. Becke AD (1993) Structure and optical properties of 2,3,7,9-polysubstituted carbazole derivatives. Experimental and theoretical studies new mixing of Hartree-Fock and local density-functional theories. J Chem Phys 98:1372–1377
30. Lee C, Yang W, Parr RG (1988) Development of the Colle-Salvetti correlation-energy formula into a functional of the electron density. Phys Rev B 37:785–789
31. Kim CH, Park J, Seo J, Park SJ, Joo T (2010) Excited state intramolecular proton transfer and charge transfer dynamics of a 2-(2′-

hydroxyphenyl)benzoxazole derivative in solution. J Phys Chem A 114:5618–5629
32. Santra M, Moon H, Park MH, Lee TW, Kim Y, Ahn KH (2012) Dramatic substituent effects on the photoluminescence of boron complexes of 2-(Benzothiazol-2-yl)phenols. Chem Eur J 18:9886–9893
33. Li H, Niu L, Xu X, Zhang S, Gao F (2011) A comprehensive therotical investigation of intramolecular proton transfer in the excited states for some newly-designed diphenylethylene derivatives bearing 2-(2-hydroxy-phenyl)-benzotriazole part. J Fluoresc 21: 1721–1728
34. Hehre WJ, Radom L, Schleyer PVR, Pople J (1986) Ab initio molecular orbital theory. Wiley, New York
35. Bauernschmitt R, Ahlrichs R (1996) Treatment of electronic excitations within the adiabatic approximation of time dependent density functional theory. Chem Phys Lett 256:454–464
36. Furche F, Rappaport D (2005) Density functional theory for excited states: equilibrium structure and electronic spectra. In: Olivucci M (ed) Computational photochemistry. Elsevier, Amsterdam, Vol 16: Chapter 3
37. Lakowicz JR (1999) Principles of fluorescence spectroscopy, 2nd edn. Kluwer, New York
38. Valeur B (2001) Molecular fluorescence: principles and applications. Wiley-VCH Verlag, Weinheim
39. Phatangare KR, Gupta VD, Tathe AB, Padalkar VS, Patil VS, Ramasami P, Sekar N (2013) ESIPT inspired fluorescent 2-(4-benzo[*d*]oxazol-2-yl)naphtho[1,2-*d*]oxazol-2-yl)phenol: experimental and DFT based approach to photophysical properties. Tetrahedron 69:1767–1777
40. Padalkar VS, Ramasami P, Sekar N (2013) A combined experimental and DFT-TDDFT study of the excited-state intramolecular proton transfer (ESIPT) of 2-(2′-hydroxyphenyl) imidazole derivatives. J Fluoresc 23(5):839–851
41. Gupta VD, Tathe AB, Padalkar VS, Patil VS, Phatangare KR, Umape PG, Ramasami P, Sekar N (2013) TDDFT investigation of the electronic structures and photophysical properties of fluorescent extended styryl push-pull chromophores containing carbazole unit. J Fluoresc 23(6):1121–1138
42. Padalkar VS, Ramasami P, Sekar N (2013) TD-DFT study of excited-state intramolecular proton transfer (ESIPT) of 2-(1,3-benzothiazol-2-yl)-5-(N, N-diethylamino)phenol with benzoxazole and benzimidazole analogues. Procedia Comput Sci 18:797–805
43. Frisch MJ, Trucks GW, Schlegel HB, Scuseria GE, Robb MA, Cheeseman JR, Scalmani G, Barone V, Mennucci B, Petersson GA, Nakatsuji H, Caricato M, Li X, Hratchian HP, Izmaylov AF, Bloino J, Zheng G, Sonnenberg JL, Hada M, Ehara M, Toyota K, Fukuda R, Hasegawa J, Ishida M, Nakajima T, Honda Y, Kitao O, Nakai H, Vreven T, Montgomery JA, Peralta JE, Ogliaro F, Bearpark M, Heyd JJ, Brothers E, Kudin KN, Staroverov VN, Kobayashi R, Normand J, Raghavachari K, Rendell A, Burant JC, Iyengar SS, Tomasi J, Cossi M, Rega N, Millam NJ, Klene M, Knox JE, Cross JB, Bakken V, Adamo C, Jaramillo J, Gomperts R, Stratmann RE, Yazyev O, Austin AJ, Cammi R, Pomelli C, Ochterski JW, Martin RL, Morokuma K, Zakrzewski VG, Voth GA, Salvador P, Dannenberg JJ, Dapprich S, Daniels AD, Farkas O, Foresman JB, Ortiz JV, Cioslowski J, Fox DJ (2010) Gaussian 09, revision C.01. Gaussian, Inc., Wallingford
44. Kawski A (1966) Push–pull (thio)barbituric acid derivatives in dye photosensitized radical and cationic polymerization reactions under 457/473 nm laser beams or blue LEDs. Acta Phys Polon 29:507–518
45. Milian B, Ort E, Hernandez V, Lopez Navarrete JT, Otsubo T (2003) Spectroscopic and theoretical study of push-pull chromophores containing thiophene-based quinonoid structures as electron spacers. J Phys Chem B 107:12175–12183
46. Kato S-i, Milan Kivala W, Schweizer B, Boudon C, Gisselbrecht J-P, Diederich F (2009) Origin of intense intramolecular charge-transfer interactions in nonplanar push–pull chromophores. Chem Eur J 15(35):8687–8691
47. Bakhshiev NG (1964) Universal intermolecular interactions and their effect on the position of the electronic spectra of molecules in two component solutions. Opt Spektrosk 16:821–832
48. Chamma A, Viallet PCR (1970) Determination du moment dipolaire d'une molecule dans un etat excite singulet. Acad Sci Ser C 270: 1901–1904
49. Kawski A (1964) Dipole moments of some naphthols in the basis and stimulus condition. Nat Sci 51:82–83
50. Biradar DS, Siddlingeshwar B, Hanagodimath SM (2008) Estimation of ground and excited state dipole moments of some laser dyes. J Mol Struct 875:108–112
51. Nowak K, Wysocki S (2008) An experimental and theoretical study of dipole moments of N-[4-(9-acridinylamino)-3-methoxyphenyl]methanesulfonamide. Spectrochim Acta A 70:805–810
52. Sharma N, Jain SK, Rastogi RC (2007) Solvatochromic study of excited state dipole moments of some biologically active indoles and tryptamines. Spectrochim Acta A 66:171–176
53. Reichardt C (2003) Solvent and solvent effects in organic chemistry third and enlarged edition. Wiley VCH Verlag GmbH & Co. KGaA, Weinheim